



ELSEVIER

Contents lists available at ScienceDirect

Corrosion Science

journal homepage: www.elsevier.com/locate/corsci



Alloying effects on oxidation mechanisms in polycrystalline Co–Ni base superalloys

F.B. Ismail^a, V.A. Vorontsov^a, T.C. Lindley^a, M.C. Hardy^b, D. Dye^{a,*}, B.A. Shollock^c

^a Department of Materials, Royal School of Mines, Imperial College, Prince Consort Road, South Kensington, London SW7 2BP, UK

^b Rolls-Royce plc, ELT-10, PO Box 31, Derby DE24 8BJ, UK

^c WMG, University of Warwick, Coventry CV4 7AL, UK

ARTICLE INFO

Article history:

Received 17 November 2016

Received in revised form

15 December 2016

Accepted 20 December 2016

Available online xxx

Keywords:

Superalloys

SIMS

STEM

Oxidation

ABSTRACT

Oxidation mechanisms in polycrystalline Co–Ni–Cr–Al–W–Ta alloys were investigated using ¹⁶O/¹⁸O isotopic tracer analysis in the focused ion-beam secondary ion mass spectrometer (FIB-SIMS). It was found that Al additions favour the formation of a continuous alumina-rich layer, that Cr indirectly improved oxidation resistance and that increasing the Co fraction resulted in poorer oxidation performance. In the alloy containing 15 at.% Cr and 10 at.% Al, the outer scale formed after 200 h oxidation at 800 °C comprised oxides less than 1 μm thick. It is concluded that protective oxide scales can be formed in Co–Ni base superalloys.

© 2016 Elsevier Ltd. All rights reserved.

1. Introduction

Increased turbine entry temperatures (TET) for improved turbine efficiency push Ni-base superalloys to their operational limits. To meet the demands of increased TET, a new generation of Ni-base superalloys are now being produced through powder metallurgy (P/M). In 2006, a new Co-base alloy family was reported with strength similar to Ni-base superalloys [1]. Sato et al. discovered that the Co–Al–W ternary system contains a L1₂ γ' phase, identified as Co₃(Al,W). The development of these alloys is motivated by their potential for (i) improved creep behaviour due to reduced γ' coarsening arising from the low diffusivity of W in the matrix, (ii) reduced freezing range and therefore enhanced castability [2] and (iii) potential for higher stacking fault energies than in Ni, and hence improved creep strengths [3–5]. Ta additions have been investigated [1,6–9], finding that it is effective for stabilisation of the γ' phase, increasing the solvus temperature [10,11]. Higher temperatures require excellent environmental degradation resistance in oxidising environments to meet the operational service life of the component. Hence, the alloys studied here include 1 at.% Ta.

One of the primary factor that limits the service life of a component for high temperature applications is oxidation, which can lead to the loss of load-bearing capacity in a component by the reduction

of metallic cross section [12]. Oxidation of Co–Al–W alloys at 800 °C typically produces a multi-layered oxide structure, with Co-rich oxide in the outer layer, a mixed oxide of Co–Cr–Al in the middle layer, whilst the inner layer is suggested to be a protective layer of Al₂O₃ [13–18]. The Al is usually depleted at the oxide/alloy interface to form a continuous layer of Al₂O₃ on the surface. The effects of alloying elements on oxidation behaviour have been investigated in [8,13,11,10,14,18,15,19].

In practice, in many applications the oxidation of metals is managed rather than prevented. Protection of the underlying metal is most often accomplished by the formation of a continuous scale over the surface such that it serves as a barrier between the remaining underlying, unoxidized metal and the environment. Long-term protection is generally associated with a scale that slowly grows whilst simultaneously providing protection from further oxygen attack and avoiding significant depletion of the strengthening precipitates [12]. Protective scale formation is more desirable than coating, as it allows for healing of the scale in the case of surface damage.

The formation of protective, dense, near-stoichiometric Al₂O₃ is desirable in the order to slow down the growth rate, controlled by oxygen diffusion. In general, although both Al and Cr additions are known to improve oxidation resistance up to 900 °C [10,11,20,17], relatively small variations in composition may result undesirable changes in the base alloy microstructure, altering the mechanical performance [3], while excessive additions of Cr may lead to a decrease in γ' stability [7]. To address this, Ni was added to a

* Corresponding author.

E-mail address: david.dye@imperial.ac.uk (D. Dye).

Co–Al–W–Cr alloy to stabilise the γ/γ' microstructure while retaining oxidation resistance [11,21,17]. Al additions are detrimental to the stability of the underlying γ/γ' microstructure and yet most importantly forms the protective internal Al_2O_3 scale. For instance, it is well known that a lower aluminum content is needed to establish and maintain an Al_2O_3 scale on M–Cr–Al alloys (where M = nickel, cobalt, or iron) than on M–Al alloys. This phenomenon is generally referred to as the third-element effect. Such an effect can be extremely important from an alloy-design viewpoint, as excessive additions of aluminum, for example, tend to depress the melting point and lead to the formation of embrittling phases [12].

Additions of Cr have been found to be beneficial up to 800 °C [22]. In isothermal oxidation tests at 800 °C and 900 °C, Cr was found to promote the protective Al_2O_3 formation due to selective Al-oxidation [23]. According to an initial suggestion by Wagner [24], the third element, e.g. chromium in M–Al alloys, acts as a getter for oxygen in the alloy during the initial stage, lowering the oxygen solubility in the alloy and preventing internal oxidation of the more reactive component, aluminum, producing external Al_2O_3 layers at lower aluminum levels than in binary M–Al alloys. Yan et al. [11] have previously studied the oxidation resistance of Co–Al–W alloys with Cr-additions and multilayer oxide scales were formed. They observed that the oxide scales exhibit a three-layered structure; the external scale consists of outer Al_2CoO_4 , a Cr-rich middle layer, and internal Al_2O_3 .

The oxidation behaviour of cobalt-base superalloys can be improved by suitable alloying strategies. For this, different alloying elements, such as nickel, aluminium, and chromium, have been added to Co–Al–W ternary alloys in varying amounts to improve the oxidation behaviour. Since the current understanding of the oxide formation mechanism in Co–Al–W alloys is limited, there is a need to focus on the difference in the oxidation sequence with varying alloy content. The present study evaluates the effects of alloying, particularly Ni, Al and Cr, on the oxidation behaviour of Co–Al–W superalloys. The use of oxygen isotopes to study the transport mechanism during high temperature oxide scale growth is crucial to improving the understanding of the oxide scale. Later in this paper, the effect of additions of these elements on the oxidation mechanism of the Co-base superalloys and the changes to the underlying microstructures at temperatures of 800 °C as well as long term oxidation (200–5000 h) will be discussed.

2. Experimental methods

2.1. Material preparation

The alloy powder was manufactured by vacuum induction melting and inert gas atomisation by ATI Powder Metals, Pittsburgh, PA, USA. After powder production, the material was consolidated by hot isostatic pressing (HIP) and isothermally forged by ATI Forged Products, Cudahy, WI, USA. After forging, the material was subjected to a heat treatment of 1050 °C for 30 min, above the solvus temperature of 1000 °C. Table 1 summarises the nominal compositions of alloys with varied Ni, Al, and Cr content. Note that the first two alloys have the same Co/Ni ratio whilst the third alloy has 1.3:1 Co/Ni ratio. Hence 1.3Co is utilised in the alloy abbreviation.

Table 1
Nominal compositions of the investigated alloys and utilised abbreviations.

Alloy designation	Nominal composition in at. %						γ' solvus (°C)
	Co	Al	W	Cr	Ta	Ni	
17Cr–12Al	33.5	12	3	17	1	33.5	990
15Cr–10Al	36	10	3	15	1	35	1000
1.3Co–17Cr–10Al	40	10	3	17	1	29	1010

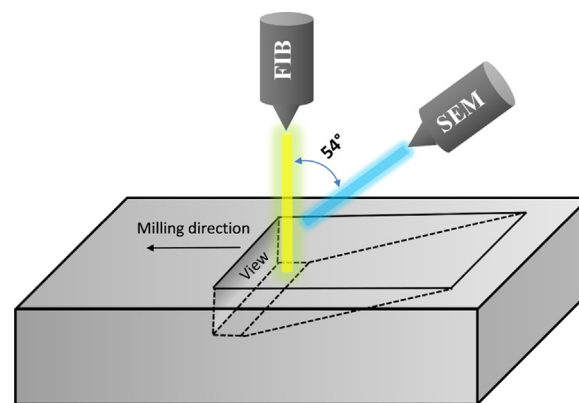


Fig. 1. Schematic of a trench FIB milling and viewing of the cross section in SEM mode.

2.2. Oxidation experiments

Oxidation experiments were carried out in an isotopic exchange oxidation rig. In order to examine the mechanism of oxide formation, two-stage experiments were carried out using oxygen-18 ($^{18}\text{O}_2$) at a partial pressure of 0.2 atm. The samples were 5 mm \times 5 mm \times 5 mm in size and surface polished to 1 μm finish using diamond suspension. The samples were first exposed to research-grade oxygen (referred to as $^{16}\text{O}_2$) at $p\text{O}_2 = 200$ mbar. The exchange furnace was evacuated before introducing the $^{18}\text{O}_2$ -enriched oxygen also at $p\text{O}_2 = 200$ mbar. The samples were then fast-cooled in air by rolling off the exchange furnace. For each exposure time, the $^{18}\text{O}_2$ -enriched oxygen was introduced during the last 24 h to act as a tracer.

Long-term isothermal oxidation experiments were conducted at 800 °C in a box furnace under atmospheric conditions. The samples were placed in alumina crucibles and exposed to laboratory air. After exposure, the samples were taken out of the furnace along with the crucibles which would contain any spalled oxide. All of the samples for both isotopic exchange oxidation and long-term isothermal oxidation were weighed before and after exposure to determine their mass change.

2.3. Characterisation

The microstructure and the chemical composition of the samples were examined using a Zeiss Auriga scanning electron microscope (SEM) equipped with an Oxford Instruments EDX detector. The morphologies of the oxide surfaces were characterised using secondary electron mode. A thin platinum strip with dimensions of 25 μm \times 2.5 μm \times 1.5 μm was deposited on the surface of each of the oxidised samples prior to milling. Trenches milled using a focused ion beam (FIB) were viewed in energy selective backscatter (EsB) mode at 36° relative to the sample surface viewing angle. SEM was chosen to capture microstructure at 1.48 kV acceleration voltage at a working distance of 5 mm, in order to identify different phases via atomic number contrast. Imaging was performed at 36° from the surface as illustrated in Fig. 1. All chemical analyses of the samples were performed using EDX in

Download English Version:

<https://daneshyari.com/en/article/5440084>

Download Persian Version:

<https://daneshyari.com/article/5440084>

[Daneshyari.com](https://daneshyari.com)